Research on an image color restoration method for old art films

H.L. Zhang [1*], C.J. Shao [2]
[1] Shanghai Dianji University, Shanghai 200240, China;
[2] Shanghai Polytechnic University, Shanghai 201209, China;
* Corresponding Author

Abstract

The preservation and restoration of old art films have certain practical value. Focusing on the color restoration of old art films, this paper introduced the same mapping loss on the basis of a cycle-consistent generative adversarial network, which enables the algorithm to capture more image details and achieve better transfer results. The old art films Roman Holiday and Tracks in the Snowy Forest were used as experimental data to verify the color restoration effect of the improved cycle-consistent generative adversarial network algorithm. It was found that compared with the generative adversarial network and cycle-consistent generative adversarial network algorithms, the improved cycle-consistent generative adversarial network algorithm was superior. It achieved a peak signal-to-noise ratio of 26.874, a structural similarity index measure of 0.665, a learned perceptual image patch similarity of 0.212, and a Frechet inception distance of 117.652 for Roman Holiday. Moreover, it achieved a peak signal-to-noise ratio of 22.794, a structural similarity index measure of 0.585, a learned perceptual image patch similarity of 0.247, and a Frechet inception distance of 119.265 for Tracks in the Snowy Forest. It also achieved better results in comparison with existing image color restoration methods. The results demonstrate the usability of the improved cycle-consistent generative adversarial network algorithm in color restoration of old art films, which can be applied in practice.

Keywords: color restoration, old art film, generative adversarial network, peak signal-to-noise ratio.
Citation: Zhang HL, Shao CJ. Research on an image color restoration method for old art films. Computer Optics 2026; 50(3): 1781. doi:10.18287/COJ1781.

Introduction

Due to the continuous advancement and innovation of related technologies such as recording, storage, and playback, the quality of films is getting higher and higher, and excellent works are emerging one after another [1]. At the same time, the preservation and restoration of old art films have also attracted widespread attention. The preservation and restoration of old art films, which carry the memories and characteristics of the time and provide inspiration and sentiment for new films, are of great value [2]. Due to the limitations of technology at that time, many of the old art films that have survived to this day have defects such as flickering and fading [3], which put a lot of pressure on artificial restoration. Digital restoration technology, with the assistance of computers, can achieve better automated restoration results [4] and is now widely used [5]. Sompoppokasest et al. [6] put forward a new type of generative adversarial network (GAN) model to remove unwanted elements from images. Experiments found that this model had high resource efficiency and requires less training time. Yuan et al. [7] designed a novel dual-U-net GAN for image restoration and found that the images restored by the designed model had reasonable texture structures for different proportions of damage. Zheng et al. [8] proposed a method for image restoration that combines smooth tucker decomposition and low-rank Hankel constraints and found that this method could achieve better peak signal-to-noise ratio (PSNR) even in extreme cases where 99 % of pixels were lost. Ning et al. [9] presented a two-stage model that fuses spatial textures and multi-stage structural features, conducted experiments under three datasets and five mask ratios, and demonstrated the effe ctiveness of the model. Andriyanov et al. [10] synthesized special modifications of nonlinear filters based on deep doubly stochastic Gaussian models. Through experiments, they found that with the help of the doubly stochastic model, the image can be restored using only 50 % of the information. Sun et al. [11] introduced LlamaGen for scalable image generation, verified the effectiveness of the LLM service framework in optimizing the inference speed of the image generation model, and found it achieved an acceleration of 326 % – 414 %. This paper studied the color restoration of old art films by designing a method with a generative adversarial network (GAN). It took the old art films Roman Holiday and Tracks in the Snowy Forest as examples to verify the restoration effect of this method, providing some references for the digital restoration of old art films, which is conducive to better preservation and inheritance of old art films.

1. Color restoration method

The fading of old art films poses a significant obstacle to their dissemination, and the dull images affect the viewer's visual experience. Image color restoration methods can be used to enhance the picture effect. Deep learning-based image processing approaches have a strong ability in feature extraction [12] and have been widely used in image restoration [13], such as convolutional neural networks [14] and Transformer [15]. Among them, the cycle-consistent generative adversarial network (CycleGAN) [16] algorithm has shown excellent performance in generating images that conform to human visual perception. Therefore, based on the CycleGAN algorithm, this paper studied the image color restoration of old art films.

The CycleGAN algorithm converts data through a generative network and a discriminative network. It mainly contains two parts of loss.

1). Adversarial loss

Adversarial loss is utilized to optimize GAN networks. For generator G: $X \to Y$, the loss function of discriminator D_Y can be written as:

$$L_{GAN}(G, D_Y, X, Y) = E_{y\sim Pdata(y)}[\ln D_Y(y)] + E_{x\sim Pdata(x)}\left[\ln\left(1 - D_Y\big(G(x)\big)\right)\right], \quad (1)$$

where $D_Y(y)$ is the probability that image y belongs to domain Y, $E_{y\sim Pdata(y)}$ is the expectation that y takes from Y, and $E_{x\sim Pdata(x)}$ is the expectation that x takes from X.

For generator F: $Y \to X$, the loss function of discriminator D_X is:

$$L_{GAN}(F, D_X, Y, X) = E_{x\sim Pdata(x)}[\ln D_X(x)] + E_{y\sim Pdata(y)}\left[\ln\left(1 - D_X\big(F(y)\big)\right)\right], \quad (2)$$

where $D_X(x)$ is the probability that image x belongs to domain X.

2). Cyclic consistency loss

The CycleGAN algorithm simultaneously performs G and F mapping. The cyclic consistency loss is:

$$L_{Cycle}(G, F) = E_{x\sim Pdata(x)}\left[\left\|F\big(G(x)\big) - x\right\|_1\right] + E_{y\sim Pdata(y)}\left[\left\|G\big(F(y)\big) - y\right\|_1\right], \quad (3)$$

where $E_{x\sim Pdata(x)}[\cdot]$ indicates that image x in domain X generates $G(x)$ under the action of generator G and $G(x)$ generates $F\big(G(x)\big)$ that is similar to image x under the action of generator F. $E_{y\sim Pdata(y)}[\cdot]$ is similar to $E_{x\sim Pdata(x)}$.

Ultimately, the target loss of the CycleGAN algorithm is:

$$L(G, F, D_X, D_Y) = L_{GAN}(G, D_Y, X, Y) + L_{GAN}(F, D_X, Y, X) + \beta L_{Cycle}(G, F), \quad (4)$$

where β is the weighting factor that controls the relative importance degree of different losses.

The CycleGAN algorithm is applied to the color restoration of old art films. To add consideration for style loss during restoration, an improvement is made based on CycleGAN. The original CycleGAN algorithm uses a cycle consistency loss that lacks consideration of the loss between the generated images and the real images. In this case, if the style loss between the generated images and the real images is significant, the subsequent image generation effect may be poor. Eventually, the generated results may appear unnatural in color or deviate in style. Therefore, to solve this problem, the same mapping loss is added based on the loss of the cycle consistency:

$$L_{Cycle}(G, F) = E_{x\sim Pdata(x)}\left[(1 - \beta_1)\left\|F\big(G(x)\big) - x\right\|_1 + \beta_1\|G(x) - y\|_1\right] + E_{y\sim Pdata(y)}\left[(1 - \right.$$
$$\left. -\beta_2)\left\|G\big(F(y)\big) - y\right\|_1 + \beta_2\|F(y) - x\|_1\right], \quad (5)$$

where β_1 is the loss weight of the $x \to G(x) \approx y$ process, $(1\text{-}\beta_1)$ is the loss weight of the $F\big(G(x)\big) \to x$ process, β_2 is the loss weight of the $y \to F(y) \approx x$ process, and $(1\text{-}\beta_2)$ is the loss weight of the $G\big(F(y)\big) \to y$ process.

Based on this, the *process* of the CycleGAN algorithm to restore the color of old art films is shown in Figure 1.

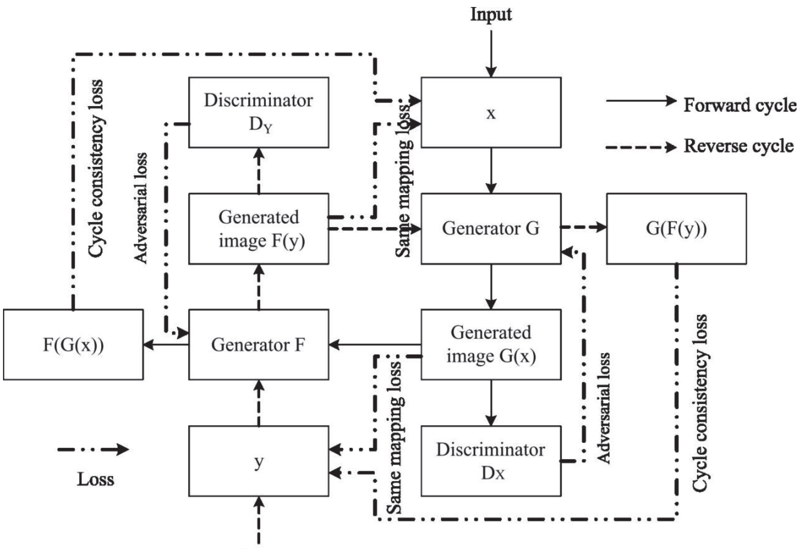

Fig. 1. Color restoration of old art films with the improved CycleGAN algorithm1

According to Figure 1, the CycleGAN algorithm follows specific steps outlined below.

3). Generate repaired image frames $G(x)$ and $G(F(y))$ based on the generative network.

4). Generate unrepaired image frames $F(y)$ and $F(G(x))$ based on the generative network.

5). Set the gradient of the generative network to 0, calculate the same mapping loss $L_{Cycle}(G, F)$ by equation (5), and perform backpropagation.

6). Update the weight parameters of generative networks G and F.

7). Use the root mean square error to calculate the gradient of discriminators D_X and D_Y and update the weight parameters.

8). Repeat the above steps until the optimal model is obtained and output color-restored image frames.

2. Experiments and analyses

2.1. Experimental setup

The experiment was conducted in a Windows 10 operating system environment. The algorithm was built using PyTorch 1.8.1. Python 3.8 was used as the programming language. After repeated experiments, the learning rate of the improved CycleGAN algorithm was set to 0.0002. The number of epochs was 100, the batch size was 8, and the initial values of β_1 and β_2 were 0.2. The experimental data were derived from the old art films *Roman Holiday* (1953) and *Tracks in the Snowy Forest* (1960), both of which had manually restored versions. Ten video sequences were selected from both the unrestored and restored films for the experiment, each containing 100 frames of images. The training set and test set were divided in an 8:2 ratio.

2.2. Evaluation indicators

The following four indicators were used to evaluate the color restoration effect of old art films.

1). Peak signal-to-noise ratio (PSRN) [17]

PSNR can be used to measure the quality of restored images with the following formula:

$$PSNR=10\log_{10}\left(\frac{255^2}{\mathrm{MSE}}\right), \tag{6}$$

where MSE is the mean square error of the two images before and after restoration.

2). Structural similarity index measure (SSIM) [18]

SSIM is employed to measure the similarity between images, and its formula is:

$$\mathrm{SSIM(A,B)}=\frac{(2\mu_A\mu_B+C_1)(2\sigma_{AB}+C_2)}{(\mu_A^2+\mu_B^2+C_1)(\sigma_A^2+\sigma_B^2+C_2)}, \tag{7}$$

where C_1 and C_2 are constants, μ_A and μ_B are the pixel mean of the images A and B, and σ_{AB} is the covariance of images A and B.

3). Learned perceptual image patch similarity (LPIPS) [19]

LIPIPS measures the similarity between images based on human perception, and its formula is:

$$\mathrm{LPIPS(A,B)}=\sum_l\frac{1}{H_lW_l}\sum_{h,w}\left\|wl\odot\left(F_A^l(h,w)-F_B^l(h,w)\right)\right\|_2^2, \tag{8}$$

where $F_A^l(h, w)$ and $F_B^l(h, w)$ are the l-th layer feature of images A and B in the pre-training network, W_l is the trainable weight parameter with temperature scaled by channel count.

4). Frechet inception distance (FID) [20]

FID measures the distance between the generated image and the real image, and its formula is:

$$\mathrm{FID(A,B)}=|\delta_A-\delta_B|^2+\mathrm{Tr}(\varphi_A+\varphi_B)-2(\varphi_A*\varphi_B^{1/2}), \tag{9}$$

where δ_A is the feature mean of the generated image, δ_B is the feature mean of the real image, φ_A and φ_B are the covariance matrix of the generated and real images, and Tr is the trace of the matrix.

2.3. Analysis of restoration results

The proposed method was compared with the GAN and CycleGAN algorithms to verify its effectiveness.

According to Table 1, the improved CycleGAN algorithm showed better performance in color restoration of old art films compared with the GAN and CycleGAN algorithms. In the case of *Roman Holiday*, the improved CycleGAN algorithm achieved the highest PSNR at 26.874, which was 4.306 higher than that of the GAN algorithm and 2.249 higher than that of the CycleGAN algorithm. Its SSIM was 0.665, which was 0.058 higher than the GAN algorithm and 0.029 higher than the CycleGAN algorithm. Its LPIPS was 0.212, which was 0.086 lower than the GAN algorithm and 0.055 lower than the CycleGAN algorithm. Its FID was 117.652, which was 94.604 lower than the GAN algorithm and 58.976 lower than the CycleGAN algorithm. These results indicated that the image frames restored by the improved CycleGAN algorithm had good quality and gave a better experience in human visual perception, demonstrating the effectiveness of the improvement made to the CycleGAN algorithm for reconstructing the colors of old art films.

Then, the CycleGAN algorithm was compared with the other two existing color restoration methods to verify its superiority.

Table 1. Comparison of restoration effects

		GAN	CycleGAN	Improved CycleGAN
Roman Holiday	PSNR	22.568	24.625	26.874
	SSIM	0.607	0.636	0.665
	LPIPS	0.298	0.267	0.212
	FID	212.256	176.628	117.652
Tracks in the Snowy Forest	PSNR	19.853	21.367	22.794
	SSIM	0.512	0.543	0.585
	LPIPS	0.284	0.251	0.247
	FID	186.325	157.821	119.265

Table 2. Comparison with existing methods1

		The Wasserstein generative adversarial network in reference [21]	The perceptual loss function-trained feed-forward network in reference [22]	Improved CycleGAN
Roman Holiday	PSNR	24.365	25.625	26.874
	SSIM	0.456	0.652	0.665
	LPIPS	0.287	0.274	0.212
	FID	215.256	210.632	117.652
Tracks in the Snowy Forest	PSNR	20.785	21.336	22.794
	SSIM	0.447	0.515	0.585
	LPIPS	0.312	0.285	0.247
	FID	210.528	214.853	119.265

According to Table 2, the improved CycleGAN algorithm outperformed the Wasserstein generative adversarial network and the perceptual loss function-trained feed-forward network in terms of all evaluation indicators. In the case of *Tracks in the Snowy Forest*, the PSNR obtained by the improved CycleGAN algorithm was 22.794, significantly higher, and the SSIM was 0.585, also significantly higher than the other two methods, indicating that the restored image frames had better quality. The LPIPS of the improved CycleGAN algorithm was 0.247 and the FID was 119.265, significantly lower than the other two algorithms, suggesting that the image frames restored by the improved CycleGAN algorithm had better visual effects. These findings further demonstrated the reliability of the improved CycleGAN algorithm in color restoration of old art films.

Figures 2 – 5 shows examples of color restoration effects of the improved CycleGAN algorithm for a frame in *Roman Holiday* and *Tracks in the Snowy Forest*.

Fig. 2. Roman Holiday before restoration

Fig. 3. Roman Holiday after restoration

Fig. 4. Tracks in the Snowy Forest before restoration

Fig. 5. Tracks in the Snowy Forest after restoration

According to Figs. 2 – 5, it can be found that after the improved CycleGAN algorithm was used to perform color restoration on the video image frames of the two works, the colors of the original black-and-white movie have been reconstructed with high quality, and the overall visual effect was good, further verifying the reliability of the method in color restoration.

3. Conclusion

In this paper, the CycleGAN algorithm was improved to achieve color restoration of video image frames in old art films, and the performance of the proposed algorithm was verified by taking *Roman Holiday* and *Tracks in the Snowy Forest* as examples. Experiments revealed that the improved CycleGAN algorithm showed good results in color restoration of old art films. Compared with other methods compared, it achieved higher PSNR and SSIM values and lower LPIPS and FID values. It suggested good color restoration effects for old art films and achieved good visual effect; thus it can be further promoted and applied in practice.

References

[1] Zheng X. Research on marketing strategies of domestic movies under the perspective of 4V theory: taking “Full River Red” as an example. SHS Web Conf 2024; 188: 03004. doi:10.1051/shsconf/202418803004.

[2] Renaudeau A, Seng T, Carlier A, Pierre F, Lauze F, Aujol JF, Durou JD. Learning defects in old movies from manually assisted restoration. In: Proc 25th Int Conf Pattern Recognit (ICPR); 2021. doi:10.1109/ICPR48806.2021.9413196.

[3] Dai M, Zhang W, Zheng W. Digital stabilization method for old movies based on MobileSAM and optical flow. Multimed Syst 2025; 31(3): 1-12. doi:10.1007/s00530-025-01740-6.

[4] Cao C, Dong Q, Fu Y. ZITS++: image inpainting by improving the incremental transformer on structural priors. IEEE Trans Pattern Anal Mach Intell 2023; 45(10): 12667-12684. doi:10.1109/TPAMI.2023.3280222. [web:398][web:399]

[5] Xian J, Xu X, Xian Y, Xian C. Image inpainting algorithm based on hybrid encoding and mask space modulation. J South China Univ Technol Nat Sci Ed 2025; 53(3): 31-39. doi:10.12141/j.issn.1000-565X.240155.

[6] Sompoppokasest S, Siriborvornratanakul T. Lightweight image inpainting model for removing unwanted objects from residential real estate indoor scenes. Multimed Tools Appl 2024; 83(34): 80389-80410. doi:10.1007/s11042-024-18605-1.

[7] Yuan J, Wu H, Wu F. Novel dual U-Net generative adversarial network for image inpainting. Int J Pattern Recognit Artif Intell 2024; 38(6): 2454006. doi:10.1142/S0218001424540065.

[8] Cai J, Jiang J, Wang Y, Zheng J, Xu H. Image inpainting via smooth Tucker decomposition and low-rank Hankel constraint. Int J Comput Appl 2023; 45(6): 421-432. doi:10.1080/1206212X.2023.2219836.

[9] Ning T, Huang G, Li J, Huang S. Complex image inpainting of cultural relics integrating multi-stage structural features and spatial textures. Pattern Anal Appl 2025; 28(2): 1-18. doi:10.1007/s10044-025-01434-9.

[10] Andriyanov N, Belyanchikov A, Vasiliev K, Dementiev V. Restoration of spatially inhomogeneous images based on doubly stochastic filters. In: Proc VIII Int Conf Inform Technol Nanotechnol (ITNT); 2022. 4 pp. doi:10.3103/S8756699022050028.

[11] Sun P, Jiang Y, Chen S, Zhang S, Peng B, Luo P, Yuan Z. Autoregressive model beats diffusion: LLaMA for scalable image generation. arXiv 2024; arXiv:2406.06525. Available at: https://arxiv.org/abs/2406.06525.

[12] Faye B, Azzag H, Lebbah M, Bouchaffra D. Adaptive context normalization: a boost for deep learning in image processing. In: Proc 2024 IEEE Int Conf Image Process (ICIP); 2024. pp. 1037-1043. (preprint: arXiv:2409.04759).

[13] Chang R, Liu G, Qian Y, Tang H, Wang G, Bavirisetti DP. GDNet: low-light image enhancement network based on Ghost-block and unique image decomposition. J Supercomput 2025; 81(1): 160. doi:10.1007/s11227-024-06683-9. [web:402]

[14] Miao J, Kou K, Yang Y, Yang L, Han J. Quaternion matrix completion using untrained quaternion convolutional neural network for color image inpainting. Signal Process 2024; 221: 109635. doi:10.1016/j.sigpro.2023.109635. (preprint: arXiv:2305.00416).

[15] Miao W, Wang L, Lu H, Huang K, Shi X, Liu B. ITrans: generative image inpainting with transformers. Multimed Syst 2024; 30(1): 1-12. doi:10.1007/s00530-023-01211-w. [web:402][web:406]

[16] Zhu JY, Park T, Isola P, Efros AA. Unpaired image-to-image translation using cycle-consistent adversarial networks. In: Proc IEEE Int Conf Comput Vis (ICCV); 2017. pp. 2242-2251. doi:10.1109/ICCV.2017.244.

[17] Anjum U, Afzal U, Hussain A, Hussain I, Channa BA, Noorwali A, Shah SA. JPEG image compression using multiple core strategy in FPGA achieving high peak signal-to-noise ratios. In: Proc Int Congr Adv Technol Eng (ICOTEN); 2021. pp. 1-6. doi:10.1109/ICOTEN52080.2021.9493460.

[18] Kang M, Baek J. SAR image change detection via multiple-window processing with structural similarity. Sensors 2021; 21(19): 6645. doi:10.3390/s21196645.

[19] Diaw M, Retraint F, Morain-Nicolier F, Delahaies A, Landre J. New statistic detector for structural image similarity. IEEE Trans Signal Process 2025; 73: 1168-1183. doi:10.1109/TSP.2025.3543207.

[20] Siddiqui AA, Tirunagari S, Zia T, Windridge D. Latent diffusion approach to visual attribution in medical imaging. Sci Rep 2025; 14(1): 962. doi:10.1038/s41598-024-81646-x.

[21] Arjovsky M, Chintala S, Bottou L. Wasserstein generative adversarial networks. Proc 34th Int Conf Mach Learn (ICML); 2017; 70: 214-223. (Conf Track Proc Mach Learn Res).

[22] Johnson J, Alahi A, Fei-Fei L. Perceptual losses for real-time style transfer and super-resolution. In: Proc Eur Conf Comput Vis (ECCV); 2016. pp. 694-711. doi:10.1007/978-3-319-46475-6_43.

About authors

Honglei Zhang (b. 1983) graduated from the Central Academy of Fine Arts in June 2015. He is working at Shanghai Dianji University as a lecturer. He is interested in fine arts. E-mail: *zhongl_zhang@hotmail.com*

Changjuan Shao (b. 1986) graduated from Shanghai University in June 2016. She is working at Shanghai Polytechnic University as a lecturer. She is interested in design. E-mail: *scjuan_shao@hotmail.com*

Received: July 21, 2025. Final version – November 17, 2025